



Photocatalytic activity of boron-modified TiO₂ under visible light: The effect of boron content, calcination temperature and TiO₂ matrix

Adriana Zaleska^{a,*}, Ewelina Grabowska^a, Janusz W. Sobczak^b, Maria Gazda^c, Jan Hupka^a

^a Department of Chemical Technology, Gdansk University of Technology, 80-952 Gdansk, Poland

^b Laboratory of Electron Spectroscopies, Institute of Physical Chemistry Polish Academy of Sciences, 01-224 Warsaw, Poland

^c Department of Solid State Physics, Faculty of Applied Physics and Mathematics, Gdansk University of Technology, 80-952 Gdansk, Poland

ARTICLE INFO

Article history:

Received 2 December 2008

Received in revised form 26 December 2008

Accepted 11 January 2009

Available online 19 January 2009

Keywords:

Titanium dioxide

Boron-modified TiO₂

Visible light photocatalysis

ABSTRACT

Our research examines the photoactivity under visible light ($\lambda > 400$ nm) and surface properties (BET surface area, UV–vis absorption properties, chemical composition and crystal structure) of boron-modified TiO₂. B–TiO₂ photocatalysts were prepared by surface impregnation procedure using boric acid triethyl ester (BATE) as a boron precursor. The photocatalytic activity of obtained powders in visible light was estimated by measuring the decomposition of phenol (0.21 mmol/dm³) in aqueous solution. The effect of boron content, calcination temperature and titanium dioxide source used during preparation procedure on photoactivity was investigated. The degradation of phenol indicated that the photoactivity under visible light strongly depended on preparation manner of B–TiO₂ photocatalysts. The highest photoactivity was observed for the sample obtained by impregnation with 2 wt.% of BATE and calcinated at 400 °C. Phenol degradation rate, in the presence of these samples, equaled to 3.0 $\mu\text{mol dm}^{-3} \text{ min}^{-1}$. The mode of BATE binding to TiO₂ surface is discussed.

© 2009 Elsevier B.V. All rights reserved.

1. Introduction

Photocatalytic reactions at the surface of titanium dioxide have been attracting much attention in view of their practical applications to environmental cleaning such as self cleaning surfaces, water, wastewater and air purification, bacteria inactivation, hydrogen generation and CO₂ photoconversion to methane and low hydrocarbons [1,2]. According to the novel approach, photocatalysts exhibiting reactivity under visible light ($\lambda > 400$ nm) could be obtained by non-metal doping such as nitrogen [3,4], sulfur [5–7], carbon [8–11], phosphorus [12,13] and boron [14–18].

Our previous investigation [17] confirmed prediction made by Xu et al. [14], that boron modification can result in absorption of visible light and that B–TiO₂ can be active in the presence of visible light. We prepared B–TiO₂ by sol–gel and by surface impregnation methods using H₃BO₃ and (C₂H₅O)₃B as boron sources. It was found that only samples prepared by surface impregnation e.g. grinding of boric acid triethyl ester with pure TiO₂ and subsequent calcinations at 450 °C, were active under visible light. The surface impregnation method allowed to introduce all modifying moieties at the surface of TiO₂ particles and they could play significant role in the surface photocatalytic reaction.

Simultaneously, B-doped and N,B-codoped TiO₂ activated under visible light was reported by In et al. [18]. In et al. prepared B–TiO₂ photocatalysts with nominal doping levels in the range 1.13–11.9 at.% by reaction of BH₃ in THF with TiCl₄ under dry, O₂-free nitrogen atmosphere, followed by TiCl₄ hydrolysis, then calcination. Maximum photoactivity occurred at 1.13% B content.

The superhydrophilicity and chemical state of boron-doped TiO₂ prepared by the ion implantation method was examined by Masahashi and Oku [19]. They found that the improvement in the superhydrophilicity by boron doping is due to the reduction of titanium, and the deterioration of superhydrophilicity with the subsequent annealing was due to the oxidation of reduced titanium and the inward diffusion of boron [19].

In this work, series of boron-modified TiO₂-based photocatalysts were prepared by surface impregnation method using boric acid triethyl ester as boron precursor. The effect of boron content, calcination temperature and TiO₂ matrix used for preparation on the photocatalyst structure, surface area, crystallinity and photoactivity under visible light were systematically investigated.

2. Experimental

2.1. Materials and instruments

TiO₂ ST-01 powder having anatase crystal structure was obtained from Ishihara Sangyo, Japan (anatase, surface area 300 m²/g, particle size 7 nm). A11 was obtained from Z.Ch

* Corresponding author. Tel.: +48 58 3472437; fax: +48 58 3472065.

E-mail address: azal@chem.pg.gda.pl (A. Zaleska).

“POLICE” SA (anatase, surface area 12 m²/g), Poland and P25 from Degussa GmbH, Germany (surface area 50 m²/g). 99% boric acid triethyl ester (BATE) and boric acid (99%) from Sigma–Aldrich Co. were used as boron source in preparation procedure, without further purification.

Gemini V (model 2365) was used to measure BET surface area of the catalysts. The S_{BET} values were calculated according to the BET method using adsorption data at relative pressure p/p_0 between 0.05 and 0.3.

The catalyst powder crystal structure was determined from XRD pattern measured in the range of $2\theta = 20\text{--}80^\circ$ using X-ray diffractometer (Xpert PRO-MPD, Philips) with Cu target ($\lambda = 1.542 \text{ \AA}$). The XRD estimation of the crystallite size was based on the Scherrer formula: $d = (0.9\lambda)/(B_e - B_i)\cos\theta$, where λ is the X-ray wavelength, B_e indicates the measured breadth of a peak profile, while B_i is the ideal, non-broadened breadth of a peak and θ is the diffraction angle. The value of B_i was estimated on the basis of the measurements performed for a standard sample of polycrystalline Si with large crystalline grains. The accuracy of the grain size analysis has been estimated to be about 20%.

The diffuse reflectance spectra DRS were characterized using UV–vis spectrometer (Specord M40, Carl Zeiss) equipped with an integrating sphere accessory for diffuse reflectance.

ESCALAB-210 spectrometer (VG Scientific) was used for X-ray photoelectron spectroscopy (XPS) measurements with the Al K α X-ray source operated at 300 W (15 kV, 20 mA). The spectrometer chamber pressure was about 5×10^{-9} mbar. The samples were pressed into pellets before measurements. Survey spectra were recorded for all the samples in the energy range from 0 to 1350 eV with 0.4 eV step. High resolution spectra were recorded with 0.1 eV step, 100 ms dwell time and 20 eV pass energy. 90° take-off angle was used in all measurements. AVANTAGE data system software served for curve fitting. The background was fit using nonlinear Shirley model. Scofield sensitivity factors and measured transmission function were used for quantification. Carbon contamination C 1s peak at 284.60 eV was used as the reference of binding energy.

2.2. Preparation of B–TiO₂ photocatalysts

Boron-modified TiO₂ photocatalysts were prepared by grinding TiO₂ powder in an agate mortar with different amounts of boric acid triethyl ester (0.23, 0.93, 2.32 and 4.64 ml). The reference sample was prepared by mixing TiO₂ with 0.93 ml of CH(OC₂H₅)₃ (ethyl orthoformate), followed by pulverization and calcination at 450 °C. The commercially available TiO₂ powders tested were: ST-01 (Ishihara Sangyo Ltd., Japan; 300 m²/g), P25 (Degussa, Germany, 50 m²/g) and A11 (Police S.A., Poland 12 m²/g). The obtained powders were dried for 24 h at temperature 80 °C and calcinated at 200, 300, 350, 400, 450 and 600 °C for 1 h in air.

2.3. Photocatalytic decomposition of phenol

The photocatalytic activity of B–TiO₂ powders visible light was estimated by measuring the decomposition rate of phenol

(0.21 mmol/dm³) in an aqueous solution. Photocatalytic degradation runs were preceded by blind tests in the absence of a catalyst or illumination.

Twenty five milliliters of catalyst suspension (125 mg) was stirred using a magnetic stirrer and aerated (5 dm³/h) prior and during the photocatalytic process. Aliquots of 1.0 cm³ of the aqueous suspension were collected at regular time periods during irradiation and filtered through syringe filters ($\phi = 0.2 \mu\text{m}$) to remove catalyst particles. Phenol concentration was estimated by colorimetric method using UV–vis spectrophotometer (DU-7, Beckman). The suspension was irradiated using 1000 W Xenon lamp (6271H, Oriel), which emits both UV and vis light. The optical path included water filter and glass filters (GG) to cut off IR and UV irradiation. To limit the irradiation wavelength, the light beam was passed through GG400 filter to cut off wavelengths shorter than 400 nm.

3. Results and discussion

3.1. The effect of boron content

The amount of boric acid triethyl ester taken for photocatalysts preparation was calculated on the assumption that the content of boron in the sample after synthesis should be equal from 0.5 to 10 wt.% of the dry mass. Sample labeling, amount of dopant used in preparation procedure as well as photocatalysts characteristics are given in Table 1. All photocatalysts obtained by grinding of ST-01 with BATE (0.5, 2, 5 and 10 wt.%) followed by calcinations at 450 °C were in the form of beige powders. Photocatalytic activity of B-doped TiO₂ powders was estimated by measuring the decomposition rate of phenol in aqueous solution in the presence of visible light irradiation ($\lambda > 400 \text{ nm}$). No degradation of phenol was observed in the absence of photocatalyst or illumination.

Photocatalytic activity under visible light is presented as phenol degradation rate (Table 1) and as efficiency of phenol removal after 60 min of irradiation (Fig. 1). The highest photoactivity was observed for sample prepared with 2 wt.% of boric acid triethyl ester. Phenol degradation rate was $2.9 \mu\text{mol dm}^{-3} \text{ min}^{-1}$ for the BE-G(2) sample, while for pure TiO₂ ST-01 degradation rate equaled $0.2 \mu\text{mol dm}^{-3} \text{ min}^{-1}$. After 60 min irradiation of aqueous suspension, initially containing 40 mg/dm^{-3} of phenol, 80% of those was degraded. For photocatalyst modified with 0.5, 5 and 10 wt.% of boric acid triethyl ester, 61%, 48% and 39% of phenol was degraded, respectively.

Usually, anion doping influences light absorption characteristics of titanium dioxide. Fig. 2 shows the absorption spectra of B–TiO₂ doped with different amount of BATE. The absorption spectra of B-doped TiO₂ samples show a stronger absorption in the UV–vis region. Experimental data clearly indicate the presence of correlation between absorption and photoactivity of the obtained powders – for increased photoactivity absorption in visible region also increased. Sample BE-G(2) – showing the highest photoactivity under visible light – revealed the best absorption in visible

Table 1
Surface properties and photoactivity under visible light ($\lambda > 400 \text{ nm}$) of B-modified TiO₂, prepared by surface impregnation of ST-01 with 0.5 to 10 wt.% of boric acid triethyl ester and subsequent calcination at 450 °C.

Sample number	Assumed content of boron (wt.%)	Band gap energy (eV)	BET surface area (m ² /g)	XPS-determined content (at.%)		Phenol degradation reaction rate ($\mu\text{mol dm}^{-3} \text{ min}^{-1}$)
				C	B	
BE-G(0.5)	0.5	3.4	160	18.5	3.2	2.7
BE-G(2)	2	3.3	183	14.6	6.6	2.9
BE-G(5)	5	3.3	180	9.8	9.7	1.7
BE-G(10)	10	3.4	158	18.4	12.3	1.5
TiO ₂ -ST-01	0	3.3	276	–	–	0.2

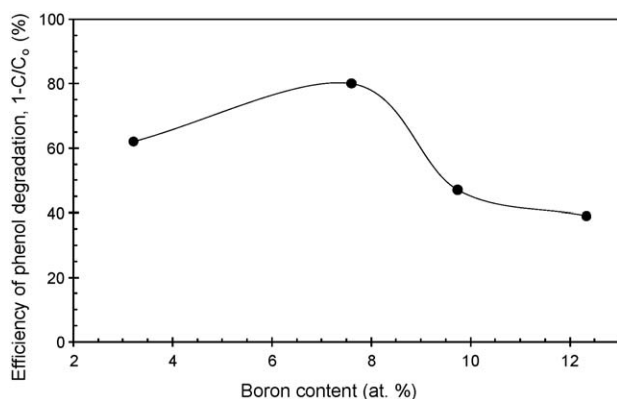


Fig. 1. Phenol degradation efficiency in the presence of B-TiO₂ photocatalysts containing different amount of boron. Boron content was presented as a surface boron content estimated by XPS analysis. Experimental conditions of phenol photodegradation: phenol initial concentration: 0.21 mM; photocatalyst loading: 125 mg; irradiation time: 60 min, temperature of reaction medium: 10 °C; air flow rate: 5 dm³/h, light spectrum: cut off by GG400 filter, $\lambda > 400$ nm.

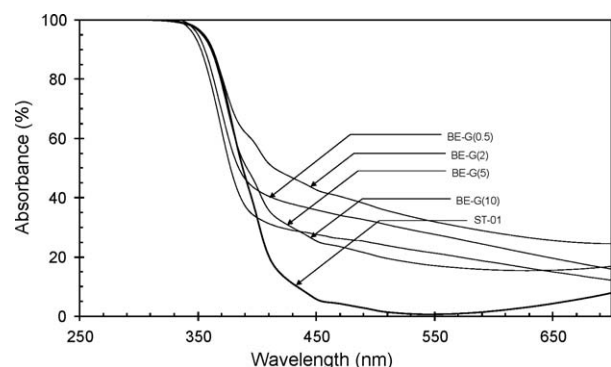


Fig. 2. Absorption properties of B-TiO₂ prepared by grinding anatase with different amount of (C₂H₅O)₃B.

region. Photoactivity and absorption properties could be listed as follows: BE-G(2) > BE-G(0.5) > BE-G(5) < BE-G(10).

The BET surface area fluctuated from 158 to 180 m²/g while the band gap (E_g) for B-TiO₂ was from 3.3 to 3.4 eV. The E_g value for the most active sample was 3.3 eV and equaled to the E_g of pure ST-01, see Table 1. We did not observe band gap narrowing in the case of boron-modified TiO₂, what is in good agreement with our previous study [17] and theoretical calculation made by Xu et al. [14].

To estimate boron and carbon influence on visible light photoactivity, additional reference sample – BE-G(0) – was prepared. Sample BE-G(0) was prepared by grinding pure TiO₂-ST-01 with 0.93 ml of CH(OC₂H₅)₃ (ethyl orthoformate) followed by calcination at 400 °C. Ethyl orthoformate was chosen as a compound with similar structure to boric acid triethyl ester, however, containing only carbon, oxygen and hydrogen atoms. Phenol degradation rate under visible light was 0.2 $\mu\text{mol dm}^{-3} \text{ min}^{-1}$ and it was much lower than phenol degradation rate for all boron-modified TiO₂ and similar to photoactivity of pure ST-01. Surface area of the BE-G(0) sample was lower than ST-01 due to shrinking during calcination. BET surface area of BE-G(0) and ST-01 was 145 and 211 m²/g, respectively.

This result confirmed our earlier investigation concerning carbon role in visible light activity. Only sample calcinated at 350 °C was active in phenol degradation in visible light (2.8 $\mu\text{mol dm}^{-3} \text{ min}^{-1}$ for $\lambda > 400$ nm) [24]. The increase of the calcination temperature to 450 °C, resulted in photoactivity

suppressing. Thus, visible light activity of the BE-G(2) sample can be rather related to the presence of boron than carbon.

Utilization of H₃BO₃ for surface impregnation also led to obtaining photocatalysts inactive under visible light [17]. Therefore, only application of boric acid triethyl ester for surface impregnation resulted in species responsible for visible light response. To investigate the surface atomic composition and chemical characters of modifying moieties, XPS analysis was performed.

Table 1 shows the content of boron and carbon of TiO₂ samples modified with 0.5–10 wt.% of BATE and calcinated at 450 °C. Boron content increased with increasing amount of BATE used for modification and ranged from 3.2 to 12.3 at.% in the surface layer. The most active sample – BE-G(2) – contained 58.4 at.% O, 19.7 at.% Ti, 14.6 at.% C and 6.6 at.% B. The boron chemical character was determined from XPS analysis. The BE-G(2) sample contained boron as a B–O–B bond (5.9 at.%) and B–O–Ti bond (0.7 at.%), while the BE-G(5) sample, exhibiting lower photoactivity, contained 9.7 at.% of boron as a B–O–B species and only 0.1 at.% as a B–O–Ti species.

Visible light activity could be enhanced by presence of carbonaceous species (C–C) occurred in highly condensed and coke-like structure, which could play the role of sensitizer to induce the visible light absorption and response. XPS analysis enabled detection of carbonaceous species on the TiO₂ surface. C=O, C–OH, and C–C_{arom.} peaks appeared at 284–289 eV, where the surface C–C_{arom.} structures were best represented (12.2 at.% for the BE-G(2) sample). Carbon content in the surface layer varies from 9.8 to 18.5 at.% and was independent of boric acid triethyl ester used for modification, see Table 1.

Someone could ask why the boron content detected in the surface layer is proportional to introduced amount of boron compounds, while we did not observe the same dependency for carbon. During the thermal treatment boron could be incorporated to TiO₂ matrix (in form of Ti–O–B bond as detected) or transformed into B₂O₃ phase but it could not be removed by formation of volatile compounds. In the case of carbon, oxidation or mineralization of organic compounds (including CO₂ and coke-like structure formation) is strictly dependent on reaction conditions such as oxygen content, temperature gradient and local temperature in the oven. It is difficult to provide the same calcination condition during annealing in the air, thus the differential level of carbon was observed.

Phenol degradation rate under visible light for as-prepared B-TiO₂ is higher than reported by others. Gombac et al. [25] reported B-TiO₂ photocatalysts activated under visible light, prepared by sol-gel method using Ti(OBu)₄ and H₃BO₃ as TiO₂ and boron precursors, respectively. The photoactivity was tested in decolouration of methyl orange (MO). The initial MO and photocatalyst concentrations were 18 mg/dm³ and 2.8 g/dm³. About 80% decolouration after 120 min of irradiation was reported. Thus, simple calculation indicates that the MO degradation rate was below 0.2 $\mu\text{mol dm}^{-3} \text{ min}^{-1}$.

3.2. The effect of calcination temperature

Photocatalyst with highest photoactivity, e.g. modified with 2 wt.% of boric acid triethyl ester was chosen for further investigation. To study the effect of calcination temperature, ST-01 was ground with 2 wt.% of boric acid triethyl ester and annealed in temperature ranged from 200 to 600 °C. Sample labeling, calcination temperature and their characteristics are presented in Table 2. For all the samples BET surface area was lower than for pure ST-01 TiO₂ and ranged from 58 to 192 m²/g. The average size of anatase crystallites was between 8.5 and 13 nm and smaller crystallite size corresponds to bigger surface area. A similar

Table 2The effect of calcination temperature on surface properties and visible light photoactivity of boron-modified TiO₂.

Sample number	Calcination temperature (°C)	Band gap energy (eV)	BET surface area (m ² /g)	Crystallite size (nm)	Rate of phenol degradation (μmol dm ⁻³ min ⁻¹)
BE-G(2)_200	200	3.3	180	8.5	0.5
BE-G(2)_300	300	3.3	113	9.1	1.6
BE-G(2)_350	350	3.4	159	8.7	2.0
BE-G(2)_400	400	3.3	192 ^a (184 ^b)	8.4	3.0 ^a (2.8 ^b)
BE-G(2)_450	450	3.3	183 ^a (180 ^b)	8.5	2.9 (2.7 ^b)
BE-G(2)_600	600	3.3	58	13	0.5

^a Value obtained for the sample revealed the best photoactivity.^b Average value calculated based on three independently prepared samples.

tendency has been also observed by other authors [26]. Band gap energy fluctuated from 3.3 to 3.4 eV. Visible light activity is presented in Fig. 3 and Table 2. B-TiO₂ samples calcinated at 200 °C showed the lowest photoactivity. Phenol decomposition rate was 0.5 μmol dm⁻³ min⁻¹ and only 12% of phenol was degraded after 60 min of irradiation in the presence of the sample calcinated at 200 °C. Since the calcination temperature was elevated from 200 °C, the increase of photoactivity was observed. Phenol degradation efficiency increased to 49% and 60% for photocatalysts calcinated at 300 and 350 °C, respectively. The highest photoactivity was observed for the sample calcinated at 400 °C. Phenol degradation rate, in the presence of these samples, equaled to 3.0 μmol dm⁻³ min⁻¹ (see Table 2). After 60 min irradiation by visible light in the presence of the sample BE-G(2)_400, 82% of phenol was removed. The most active photocatalyst, i.e. the BE-G(2)_400 sample, had the higher surface area (192 m²/g). Further increase of annealing temperature resulted in photoactivity

decrease. Phenol degradation rate was 0.5 μmol dm⁻³ min⁻¹ for the sample calcinated at 600 °C. In the presence of the BE-G(2)_600 sample phenol was degraded in 15% after 60 min of irradiation.

Fig. 4 shows the UV–vis absorption spectra of boron-doped TiO₂ calcinated at temperature ranged from 200 to 600 °C. Samples BE-G(2)_350; BE-G(2)_450 and BE-G(2)_400 show the best photo-absorption in the visible region. A significant increase in the absorption at wavelengths shorter than 400 nm can be assigned to the intrinsic band gap absorption of TiO₂. The absorption spectra of B-doped TiO₂ samples show a stronger absorption in the UV–vis region.

XRD was used to investigate the phase composition and crystal structure of the as-prepared TiO₂ powders. Fig. 5 shows the effects of calcination temperature on the phase structure of the TiO₂ powders modified with 2 wt.% of boron. All diffraction peaks of the calcinated powders were indexed to pure anatase phase of TiO₂. It is in agreement with others. Moon et al. reported that for samples doped with boric acid triethyl ester diffraction lines attributed to the rutile phase of B-TiO₂ appeared when calcination temperature was 700 °C. They increased in intensity at 900 °C, where only the diffraction lines attributed to the rutile were observed [16]. Jung et al. observed that B₂O₃–SiO₂/TiO₂ samples had pure anatase phase and no rutile phase was formed even though the calcination temperature was over 900 °C [27]. For pure TiO₂ obtained by sol–gel method, phase transformation from anatase to rutile started when TiO₂ was heated up to 500 °C and above [17,20–21]. Thus, addition of BATE slowed anatase to rutile transformation. It should also be noted that our previous investigations showed that boron doping during TiO₂ photocatalyst preparation by the sol–gel method inhibited transformation from amorphous to the anatase structure [17].

In our earlier study, XRD analysis confirmed the presence of crystalline B₂O₃ in the sample prepared by grinding ST-01 TiO₂ with 10 wt.% of boron using boric acid or boric acid triethyl ester as a boron source [17]. However, the B₂O₃ structure was not observed

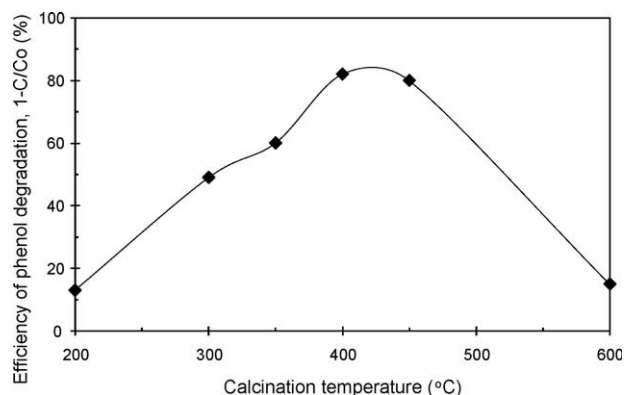


Fig. 3. Effect of calcination temperature on photocatalytic activity for TiO₂ modified with 2 wt.% of boric acid triethyl ester (BE-G(2) series). Experimental conditions of phenol photodegradation: phenol initial concentration: 0.21 mM; photocatalyst loading 125 mg; irradiation time: 60 min, temperature of reaction medium: 10 °C; air flow rate: 5 dm³/h, light spectrum: cut off by GG400 filter, λ > 400 nm.

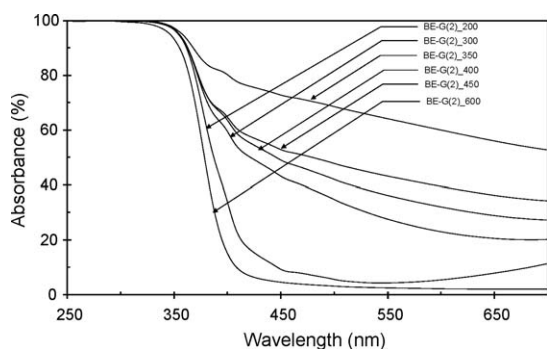


Fig. 4. The influence of calcination temperature on absorption properties of B-TiO₂ prepared by grinding anatase with 2 wt.% of (C₂H₅O)₃B.

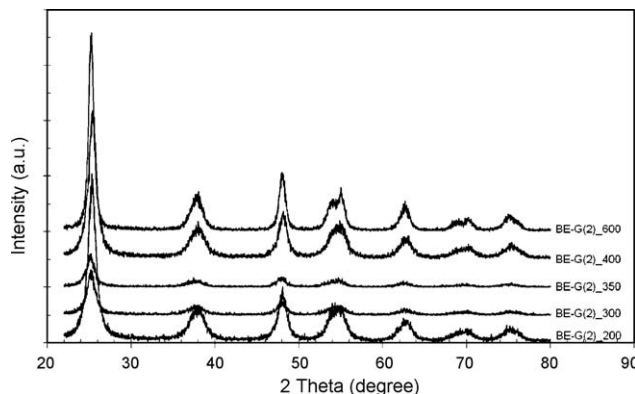


Fig. 5. XRD pattern of photocatalysts modified with 2 wt.% of (C₂H₅O)₃B and calcinated at temperature from 200 to 600 °C.

Table 3

Atomic composition and chemical characters of elements in surface layer of B–TiO₂ prepared by surface impregnation of ST-01 with 2 wt.% of boric acid triethyl ester followed by calcination at 400 °C.

Sample number	XPS-determined surface content (at.%)								
	Ti				Σ O (529.9–532.7 eV)	C	B		
	Σ Ti	Ti ⁴⁺ (458.6 eV)	Ti ³⁺ (456.8 eV)	Ti ⁴⁺ /Ti ³⁺ ratio			Σ B	B–O–B (~191.9 eV)	B–O–Ti (~193.2 eV)
BE-G(2)_200	18.8	18.2	0.6	30	58.0	12.6	8.0	7.5	0.5
BE-G(2)_300	19.2	18.2	1.0	18	59.0	12.2	6.8	6.6	0.2
BE-G(2)_350	19.0	17.9	1.0	17	54.1	18.6	6.5	6.4	0.1
BE-G(2)_400	18.9	17.2	1.7	10	55.9	16.9	6.6	6.1	0.5
BE-G(2)_450	19.7	18.3	1.4	13	54.8	14.6	6.6	5.9	0.7
BE-G(2)_600	20.1	18.4	1.8	10	59.1	11.4	7.6	7.2	0.4

for any sample modified with 2 wt.% of boric acid triethyl ester in the present study.

Table 3 shows atomic composition and chemical characters of elements incorporated in the surface layer of B–TiO₂ calcinated at 200–600 °C. The Ti 2p spectrum could be resolved into two components at binding energies ~458.6 eV and ~456.8 eV and are identified with TiO₂ and Ti₂O₃, respectively. Intensities of the decomposed components suggest that Ti⁴⁺ is the dominant surface state. An increase of the calcination temperature from 200 to 600 °C resulted in increasing amount of Ti³⁺ form. The BE-G(2)_200 sample contains Ti⁴⁺ mainly and the least amount of reduced species in the form of Ti³⁺ ions. For TiO₂ annealed at temperatures from 200 to 600 °C, the Ti⁴⁺:Ti³⁺ the ratio was from 30:1 to 10:1, respectively (see Table 3). The lowest Ti⁴⁺:Ti³⁺ (10:1) ratio was observed for TiO₂ sample calcinated at medium (400 °C) and highest temperature (600 °C).

Fig. 6A shows the XPS B 1s spectra of B–TiO₂ photocatalysts prepared by surface impregnation by 2 wt.% of boric acid triethyl ester followed by calcination at 200–600 °C. For B–TiO₂, the B 1s appeared at around 192–193 eV. Surface boron content differed from 6 to 8 at.%, see Table 4. The standard binding energy of B 1s in B₂O₃ or H₃BO₃ equals to 193.0 eV (B–O bond) and in TiB₂ equals to 187.5 eV (B–Ti bond) [22]. Our observed B 1s peak consists of two peaks. The first peak (193.2 eV) is related to B–O–Ti bonds and the second peak (191.9 eV) is related to B–O–B bonds. Thus, XPS analysis confirmed that surface impregnation combined with thermal treating allowed for incorporation of boron atoms into TiO₂ matrix.

Comparison of XPS spectra for O 1s region for samples calcinated from 200 to 600 °C is provided in Fig. 6B. O 1s peak could be composed of 3–5 different species, such as Ti–O bonds in TiO₂ and Ti₂O₃, hydroxyl groups, C–O bond, and adsorbed H₂O [23]. In our investigation four peaks were identified for sample BE-G(2)_300 and three peaks were identified for other samples. The first peak at about 532.7 eV was related to oxygen in Ti–O–B bond, the second peak at about 531.7 eV was related to surface hydroxyl groups (Ti–OH bond) and the peak at about 529.9 eV (assigned as a fourth peak in Fig. 6B) indicated oxygen in the TiO₂ crystal lattice. The asymmetry of the peak O 1s (around 533 eV), observed for all samples modified with 2 wt.% of (C₂H₅O)₃B, was also observed in our previous investigation [17] for sample prepared by surface impregnation of ST-01 TiO₂ with 10 wt.% of BATE. The peak assigned as a third peak in Fig. 6B has binding energy at 531.1 eV and appeared only for sample calcinated at 300 °C.

Our observation was in good agreement with Chen et al. and Jung et al. investigation. FTIR and XPS results obtained by Chen et al. [15] revealed that the doped boron was present as the form of B³⁺ in B-doped TiO₂ samples, forming a possible chemical structure like Ti–O–B, which was confirmed in our investigation. Jung et al. reported that the boron incorporation of SiO₂/TiO₂ mixed oxides creates structural defects such as O[–] and Ti³⁺, and the photoactivity varies with the content of boron oxide. FTIR analysis showed that boron was incorporated into the framework of titania matrix with replacing Ti–O–Si with Si–O–B or Ti–O–B [26].

In all 2 wt.% B-modified TiO₂ samples we observed the peak attributed to C 1s at around 289–284 eV. In most cases, the C 1s

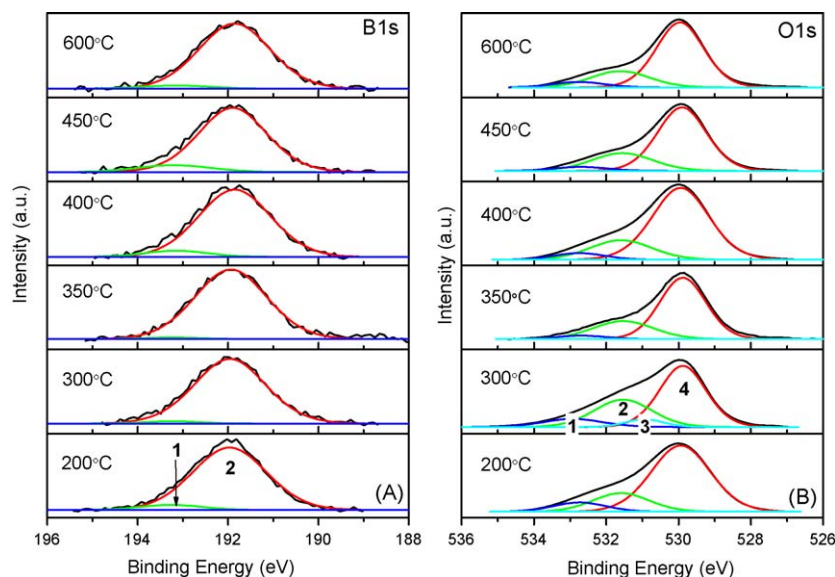


Fig. 6. XPS spectra of the TiO₂ modified with 2 wt.% of boric acid triethyl ester and calcinated at different temperatures: (A) B 1s region and (B) O 1s region.

Table 4Characteristics of TiO₂ samples used for B–TiO₂ preparation.

Sample name	Manufacturer	Surface area ^a (m ² /g)	Particle size ^a (nm)	Crystal structure ^a	Band gap ^b (eV)	BET surface area ^b (m ² /g)	Phenol degradation reaction rate under visible light ^b (μmol dm ⁻³ min ⁻¹)
A11	Police, Poland	12	No data	Anatase	3.32	12	0.2
P25	Degussa, Germany	50 ± 15	21	Anatase:rutile (80:20)	3.15	58	0.8
TiO ₂ ST-01	Ishihara Sangyo, Japan	300	7	Anatase	3.27	276	0.2

^a Data provided by manufacturer.^b As-measured.**Table 5**The effect of TiO₂ matrix on surface properties and photoactivity of B–TiO₂.

Sample number	TiO ₂ matrix	Band gap energy (eV)	BET surface area (m ² /g)	XPS-determined content (at.%)		Phenol degradation reaction rate (μmol dm ⁻³ min ⁻¹)
				C	B	
BE-G(2)_A11	A11	3.3	2.6	3.9	11.8	0.3
BE-G(2)_P25	P25	3.1	48	8.0	7.6	0.3
BE-G(2)_ST-01	ST-01	3.3	192	16.9	6.6	3.0

region consists of three peaks. The first peak (~288.9 eV) is related to COOH groups bonds, the second peak (~286 eV) to C–OH bonds and the third peak (~284.6 eV) is related to C–C aromatic bonds. Carbon content in the surface layer varies from 11.4 to 18.6 at.%, see Table 3. We did not observe correlation between total surface carbon content and visible radiation-induced activity but photocatalysts containing 12.2–14.2 at.% of carbonaceous C–C_{arom.} species clearly showed better activity (see Tables 2 and 3).

The visible light activity of the sample BE-G(2)_400 was similar to activity of S,N-doped TiO₂ under visible light described in our previous paper [28]. N,S-doped TiO₂ was obtained by hydrolysis of titanium(IV) isopropoxide with thiourea (as a nitrogen and sulfur precursor), followed by calcination at 450 °C. Phenol degradation rate under visible light in the presence of S,N-TiO₂ was 2.9 μmol dm⁻³ min⁻¹ [28], while in the presence of the most active B–TiO₂ sample was 3.0 μmol dm⁻³ min⁻¹. For photoactivity measurements of N,S- and B-modified photocatalysts, the same experimental set-up and phenol degradation conditions were used.

3.3. The effect of TiO₂ matrix

Tables 4 and 5 show the characteristics of used TiO₂ and boron-modified TiO₂ prepared using three types of TiO₂ matrix: A11 (12 m²/g), P25 (58 m²/g) and ST-01 (276 m²/g). 2 wt.% of BATE was used for surface impregnation and calcination was carried out at 400 °C for 1 h. Surface area of obtained B-modified TiO₂ was lower comparing to surface area of parent TiO₂ and equaled to 2.6, 48 and 192 m²/g for BE-G(2)_A11, BE-G(2)_P25 and BE-G(2)_ST-01, respectively. The band gap energy for samples: BE-G(2)_A11, BE-G(2)_P25, BE-G(2)_400 was 3.3, 3.2 and 3.3 eV, respectively. Optical properties of B-modified TiO₂ are presented in Fig. 7. We did not observe any increase in absorption for the samples based on A11 and P25 (absorption spectra for pure A11, P25 and ST-01 are not shown).

According to the results of XPS, as shown in Table 5, boron amount present at the surface differed from 6.6 to 11.8 at.%. Bigger difference in distribution of boron at photocatalysts surface – compare to BE-G(2) series described in previous section – could have resulted from the difference in surface area. The photocatalytic activity is shown in Table 5 and Fig. 8. Only the sample prepared using ST-01 was active under visible light. Moreover, in case of P25 surface modification resulted in decrease of photo-

activity. Slight activity under visible light of pure P25 TiO₂ can be related to the presence of the rutile phase. After 60 min of irradiation in the presence of the B–TiO₂ photocatalysts obtained from ST-01, A11 and P25, phenol was degraded in 88%, 10% and 7%, respectively. Therefore, ST-01 was found as the best manner for the TiO₂ modification, while the usage of titanium dioxides with lower

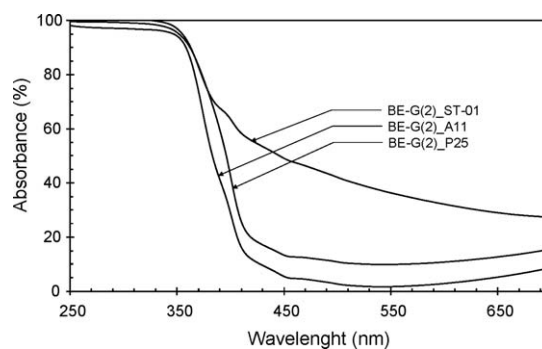


Fig. 7. Absorption properties of B–TiO₂ prepared by grinding different crystalline titanium dioxide powder with (C₂H₅O)₃B.

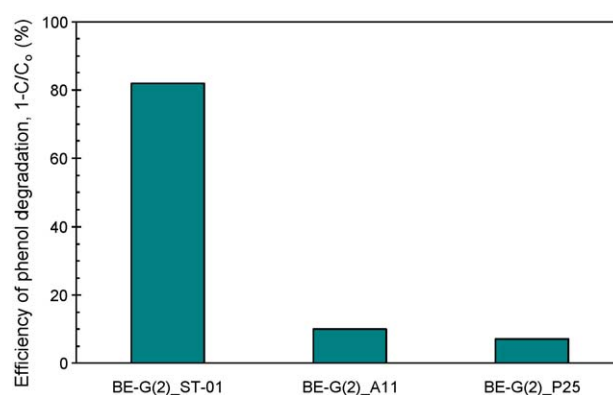


Fig. 8. The influence of titanium dioxide matrix on photoactivity in the visible light of B–TiO₂ photocatalyst containing 2 wt.% of boron. Experimental conditions of phenol photodegradation: phenol initial concentration: 0.21 mM; photocatalyst loading 125 mg; irradiation time: 60 min, temperature of reaction medium: 10 °C; air flow rate: 5 dm³/h, light spectrum: cut off by GG400 filter, λ > 400 nm.

surface area for impregnation procedure, led to rapid decrease in photoactivity.

3.4. The role of BATE in surface impregnation method

Our current and previous investigation, indicated that 0.5–5 wt.% of boric acid triethyl ester used for TiO_2 surface modification, resulted in formation of Ti–O–B bonds and increasing photoactivity under visible light. For 10 wt.% of BATE used during impregnation procedure, boron partly existed as boron oxide, what suppresses photoactivity. It is in good agreement with Jung et al. [29] investigation. For B_2O_3 – SiO_2 /TiO₂-type photocatalyst calcinated at lower temperature, they observed that the surface was covered by amorphous boron oxide. With increasing the calcination temperature, boron oxide melted and penetrated into the matrix of silica-titania resulting in increase of photoactivity under UV light.

Jung et al. [29] confirmed by EPR and FTIR analysis that more bulk defects were formed by substitution of boron into the titania framework. According to their hypothesis, the formation of bulk Ti^{3+} by the substitution of boron into anatase matrix could affect the photoactivity because it acts as an active site helping the adsorption of reactant or recombination center for photoexcited electron and hole pairs. They found, that boron content below 5%, resulted in enhancement of the photoactivity of B_2O_3 – SiO_2 /TiO₂ and boron content over 5% was responsible for deterioration of photoactivity since more bulk Ti^{3+} sites were produced.

It was found that boric acid triethyl ester is a very sensitive molecule which permits the detection of Lewis basic sites on the solid surface [30–32]. Adsorption of BATE on high-surface-area silica was studied by FTIR spectroscopy by Liu et al. [31]. It was found that surface hydroxyls remaining after outgassing at high temperatures act as weak basic sites for BATE adsorption. Coordinate interaction of BATE with isolated hydroxyls dominates the adsorption and induces two splitting B–O vibrational bands at 1375 and 1345 cm^{-1} . This result indicated that BATE may interact with isolated hydroxyl groups at oxide surface. BATE was also found to interact with basis sites of strong medium and weak basicity on alumina [32].

Thus, in the first step of our procedure, BATE could be effectively adsorbed at Lewis basic sites, such as Ti^{3+} or surface hydroxyl group over TiO_2 . Calcination step occurred to thermal decomposition of boric acid triethyl ester and incorporation of boron atoms into TiO_2 matrix. The ion radius of B^{3+} (2.0 nm) is smaller than that of Ti^{4+} (6.4 nm), so boron atom could be easily incorporated into the framework of titania [29].

To investigate thermal decomposition of BATE, derivatographic analysis of sample prepared by grinding of ST-01 with 2 wt.% of BATE was performed. Derivatographic measurements showed a weight loss occurring at 192 and 304 °C. Thus, organic part of BATE is mineralized and released as a CO and CO_2 .

4. Conclusion

We have succeeded in preparing B-modified TiO_2 photocatalysts by using a simple surface impregnation method. This

approach can efficiently introduce boron as a B–O–Ti species in the surface of TiO_2 grains. The highest photoactivity was obtained when ST-01 (Ishihara, Japan) was used as TiO_2 matrix, weight ratio of TiO_2 to boric acid triethyl ester during preparation was 50:1 and temperature at thermal treating step was 400 °C. The obtained photocatalyst showed 10 times exceeded visible light photocatalytic activity than pure TiO_2 that will be useful in the design of solar-driven photocatalytic treatment system.

Acknowledgments

This work was supported by Gdansk University of Technology (contract no. BW 014694/039) and Ministry of Science and Higher Education (contract no. N N523 483334). Dr. Beata Tryba (Department of Water Technology and Environmental Engineering, Szczecin University of Technology) is gratefully acknowledged for guidance of one of authors (E.G.) in UV-vis/DR spectroscopy.

References

- [1] A. Fujishima, X. Zhang, C.R. Chim. 9 (2006) 750–760.
- [2] M.R. Hoffmann, S.T. Martin, W. Choi, D.W. Bahnemann, Chem. Rev. 95 (1995) 69–96.
- [3] Y. Nosaka, M. Matsushita, J. Nishino, A. Nosaka, Sci. Technol. Adv. Mater. 6 (2005) 143–148.
- [4] Z. Wang, W. Cai, X. Hong, X. Zhao, F. Xu, Ch. Cai, Appl. Catal. B 57 (2005) 223–231.
- [5] T. Umebayashi, T. Yamaki, S. Tanaka, K. Asai, Chem. Lett. 32 (2003) 330–331.
- [6] T. Ohno, T. Mitusi, M. Matsumara, J. Water Sci. Technol. 49 (2004) 159–163.
- [7] T. Ohno, M. Akiyoshi, T. Umebayashi, K. Asai, T. Mitusi, M. Matsumara, Appl. Catal. A 265 (2004) 115–121.
- [8] Ch. Lettmann, K. Hildenbrand, H. Kisch, W. Macyk, W. Maier, Appl. Catal. B: Environ. 32 (2001) 215–227.
- [9] H. Kisch, S. Sakthivel, Angew. Chem. Int. Ed. 42 (2003) 4908–4911.
- [10] Y. Li, D. Hwang, N.H. Lee, S. Kim, Chem. Phys. Lett. 404 (2005) 25–29.
- [11] M. Shen, Z. Wu, H. Huang, Y. Du, Z. Zou, P. Yang, Mater. Lett. 60 (2006) 693–697.
- [12] L. Kőrösi, I. Dékány, Colloid Surf. A: Physicochem. Eng. Aspects 280 (2006) 146–154.
- [13] Z. Wang, H. Shui, J. Mol. Catal. A: Chem. 263 (2007) 20–25.
- [14] T. Xu, Ch. Lu, Y. Liu, G. Han, Science B 7 (2006) 299–303.
- [15] D. Chen, D. Yang, Q. Wang, Z. Jiang, Ind. Eng. Chem. Res. 45 (2006) 4110–4116.
- [16] S. Moon, H. Mametsuka, S. Tabata, E. Suzuki, Catal. Today 58 (2000) 125–132.
- [17] A. Zaleska, J.W. Sobczak, E. Grabowska, J. Hupka, App. Catal. B: Environ. 78 (2007) 92–100.
- [18] S. In, A. Orlov, R. Berg, F. Garcia, S. Pedrosa-Jimenez, M.S. Tikhov, D.S. Wright, R.M. Lambert, J. Am. Chem. Soc. 129 (2007) 13790–13791.
- [19] N. Masahashi, M. Oku, Appl. Surf. Sci. 254 (2008) 7056–7060.
- [20] R. Asahi, T. Morikawa, T. Ohwaki, K. Aoki, Y. Taga, Science 293 (2001) 269–271.
- [21] H. Geng, S. Yin, X. Yang, Z. Shuai, B. Liu, J. Phys. Condens. Matter 18 (2006) 87–96.
- [22] C. Su, B.Y. Hong, C.M. Tseng, Catal. Today 96 (2004) 119–126.
- [23] J. Yu, X. Zhao, Q. Zhao, Thin Solid Films 379 (2000) 7–14.
- [24] P. Górski, A. Zaleska, E. Kowalska, T. Klimczuk, J.W. Sobczak, E. Skwarek, W. Janusz, J. Hupka, Appl. Catal. B 84 (2008) 440–447.
- [25] V. Gombac, L. De Rogatis, A. Gasparotto, G. Vicario, T. Montini, D. Barreca, G. Balducci, P. Fornasiero, E. Tondello, M. Graziani, Chem. Phys. 339 (2007) 111–123.
- [26] S. Bakardjeva, J.S. Subrt, V. Stengl, M.J. Dianez, M.J. Sayagues, Appl. Catal. B 58 (2005) 193–202.
- [27] K. Jung, S. Park, S. Ihm, Appl. Catal. B 51 (2004) 239–245.
- [28] A. Zaleska, P. Górski, J.W. Sobczak, J. Hupka, Appl. Catal. B 76 (2007) 1–8.
- [29] K.Y. Jung, S.B. Park, S.K. Ihm, Appl. Catal. B 51 (2004) 239–245.
- [30] F. Koali, T. Sasaki, F. Mizukami, M. Watanabe, C. Martin, V. Rives, J. Mater. Chem. 11 (2001) 841–845.
- [31] J. Liu, P. Ying, Q. Xin, C. Li, Zeolites 19 (1997) 197–199.
- [32] J. Liu, P. Ying, Q. Xin, C. Li, Appl. Spectrosc. 53 (1999) 40.